

Morphological and nanomechanical properties of the fibrin network during coagulation and lysis

PhD Thesis

Dr. Tímea Feller

Semmelweis University
Doctoral School of Basic and Translational Medicine



Supervisor: Miklós Kellermayer, D.Sc.
Official reviewers: Levente Kiss, PhD
Attila Gergely Végh, PhD
Head of the Final
Examination committee: Zoltán Prohászka, D.Sc.
Members of the Final
Examination Committee: Orsolya Dobay, PhD
László Grama, PhD

Budapest
2019

1 Introduction

Fibrin network is the three-dimensional scaffold of the blood clot, thereby plays an important role in hemostasis. The complex spatial hierarchy of the network severely complicates the investigation of the structural and mechanical features. Consequently, neither the exact structure of the protofibrils inside the fiber, nor the exact mechanisms of the fibrinolysis are known.

The 3D fibrin network is formed after the proteolytic cleavage of fibrinogen to fibrin, followed by a spontaneous polymerisation. Fibrin monomers first form a half staggered, double-stranded structure called protofibril. Protofibrils then aggregate laterally to form fibrin fibers. The mechanism of the lateral aggregation is mostly unknown, so are the driving forces and the involved structural motifs. Based on AFM images, the α C region of the fibrin monomers can play an important role in the lateral aggregation.

Much is known about the structure and the mechanical properties of the fibrin monomer, thus the mechanical properties of the fibrin network remain mostly unknown. The mechanical properties of a network differ from the mechanical properties of the monomers and the individual fibers, even if it is partially estimated by them. The complex mechanical properties of the fibrin network can be investigated by rheological methods and thrombelastography.

2 Objectives

My aims during my PhD work were the followings.

1. To investigate nanoscale changes in the viscoelasticity of the 3D-fibrin network during coagulation by using a novel, atomic-force-microscope (AFM)-based application of force spectroscopy, named nano-thrombelastography.
2. To investigate nanoscale changes in the viscoelasticity during streptokinase (STK)-induced fibrinolysis
3. To develop a quasi-two-dimensional (2D) fibrin matrix that enables the investigation of the microstructure of the fibrin network by AFM-based topographical analysis.
4. Examine the morphological properties of fibrin in dependence of the applied NaCl concentration and thrombin activity.
5. Uncover the molecular mechanisms of the fibrinolysis by following the changes in the topology of an individual fibrin fiber during lysis.

3 Methods

3.1 Investigation of the mechanical properties of the fibrin network made from plasma samples: nano-thrombelastography (nTEG)

We added 100 μl normal mixed human plasma to 200 μl Hepes buffer (containing 10 mM Hepes, 150 mM NaCl). We initiated the clotting by the addition of CaCl_2 in the final concentration of 5 mM. Then we pipetted the 300 μl droplet on a glass slide, inside a circle with 15 mm inner diameter lined with parafilm. Then we put the slide in the sample holder of an MFP-1D AFM (Asylum Research, Santa Barbara, CA). For the measurement we used MSCT-AUHW cantilever (Bruker, Billerica, MA, USA), that was completely immersed in the droplet during the measurement. Before each measurement we estimated the spring constant of the cantilever by thermal calibration. The spring constants of the cantilevers ranged between 0,05 - 0,2 N/m. During the measurement the cantilever was moved up and down on 1 μm distance with a speed between 0,25 - 2,5 $\mu\text{m/s}$. We evaluated the data with Igor Pro 5.05S software.

3.2 Fibrinolysis followed with nTEG

We initiated the lysis of the clot, that was formed during the measurement, by the addition of streptokinase (STK). The activity of the enzyme ranged between 300-10000 IU. The clot was lysed typically in 40-60 min on room temperature,.

3.3 Preparation and lysis of the quasi-2D fibrin network

In order to prepare the fibrin network, we incubated a fibrinogen aliquot on 37 °C for 30 min, then diluted with Hepes buffer to the concentration of 2 mg/ml. We also diluted the thrombin solution with Hepes buffer to 50 IU/ml and stored it on ice until further use. Right before we initiated the clotting, we added CaCl₂ to the fibrinogen solution and diluted thrombin further to 2 IU/ml. We mixed 10 µl fibrinogen solution with 10 µl thrombin solution on a mica with 12 mm diameter and 1,13 cm² area, thereby the activation of fibrinogen and the clotting happened right on the mica surface. The final sample contained 1 mg/ml fibrinogen, 1 IU thrombin, 5 mM calcium and 150 mM NaCl. Clotting was allowed to proceed for at least 90 min at 25 °C in a humid, closed environment. Then the sample was first dried gently on the surface with nitrogen gas, then washed with high purity water and dried with nitrogen gas again.

Prior to lysis we incubated the sample with 50 µl Hepes buffer for 10 min in order to rehydrate the fibrin network. We initiated the lysis by the addition of further 50 µl solution containing plasmin. The activity of plasmin varied per measurement. Once the lysis was initiated, we loaded the sample into the AFM immediately for analysis. For further analysis, the sample was washed with high purity water and dried with nitrogen gas.

3.4 AFM imaging of the quasi-2D fibrin network

AFM images were acquired with Cypher S or ES atomic force microscope (Asylum Research, Santa Barbara, CA). We scanned the dried samples with silicon-nitride cantilevers (OTESPA-R3, Bruker, Billerica, Massachusetts) with a relatively high, 1 V free amplitude and 0.7 V setpoint. To follow fibrinolysis, a BL-AC40TS-C2 cantilever (Olympus, Tokyo, Japan) was immersed into the droplet containing plasmin. The free amplitude and the setpoint was relatively low in these measurements, 300 mV and 220 mV respectively. We analyzed the images with the software toolkit of the AFM driver program (Igor Pro 6.34 A). We measured the fiber height on cross-sectional topographical profiles, as the distance between the maximal height and the mica surface. We measured the fiber width on the cross-sectional profile at the half maximum of the height (FWHM, full width at half maximum), to make a correction for the artificial widening of the fibers.

3.5 Statistical comparison of fiber morphology

As clotting is an enzymatic reaction, the distribution of the height and the width of the fibers can vary in different experiments. Thus for comparative measurements we examined the changes on one given sample. We did not assume the standard deviation for our data, so we choose the Welch-test for the statistical comparison of the samples. As a condition of the Welch t-test, the variables should be of normal distribution but the standard deviations are not necessarily the same. Due

to the nature of our measurements we accepted these conditions. The null hypothesis of the test is that the expected values are the same. The probability of the matching is given by the p-value: the smaller the p-value, the smaller the probability of matching for the given samples.

4 Results

We investigated the nanoscale changes in the viscoelastic properties of the 3D fibrin meshwork during clot formation and fibrinolysis. We investigated the morphology of the fibrin meshwork before, during and after the lysis.

4.1 Investigation of the mechanical properties of the fibrin network with nTEG (T1)

The fibrin network formed during the clotting process caused a deflection in the up-and-down travel of the cantilever. We converted the deflection into force using the spring constant of the cantilever (**Fig. 1 part a**). The force difference (ΔF , **Fig. 1 part b**) was measured between the maximum and the minimum of each cycle and it corresponds to the strength of the clot at a given time. The pull and release curves did not follow the same trajectory, resulting a hysteresis. The area of the hysteresis is proportional to the energy dissipated by the clot and refers to a viscous behavior.

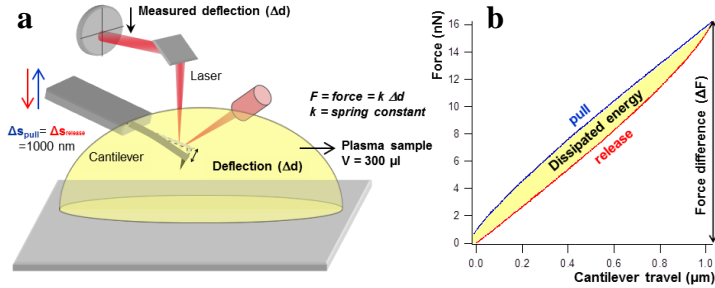


Fig. 1. Schematic model of the nTEG (a). A force vs. cantilever travel curve measured in each up-and-down travel cycles (b).

We calculated the force difference (nN) and the dissipated energy (J) for consecutive movement cycles and followed the changes of these parameters during the clotting process. Both parameters oscillated around 0 value prior to clotting, then showed a non-linear increase and reached a plateau (Fig.2.).

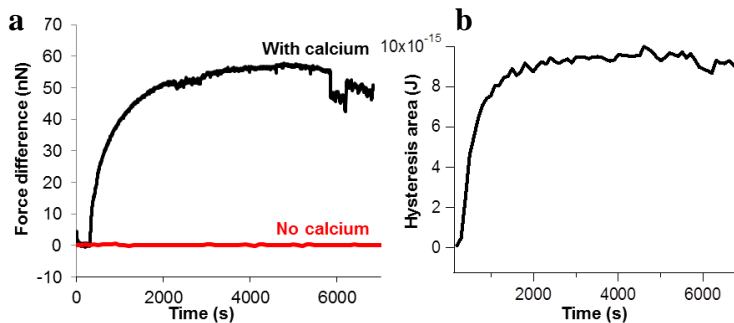


Fig. 2. nTEG curves representing the changes in the force difference (a) and dissipated energy (b) with time.

Based on 7 measurements, the average maximal force difference (where the value reached a plateau) was 21 nN ($\pm 16,5$ nN SD) and the average delay time of the coagulation (time until reaching the plateau) was 1274 s (± 597 s SD). Oscillating the cantilever in a plasma sample with no Ca^{2+} activation showed a force difference around 0 and did not increase with time (**Fig.2. part a**).

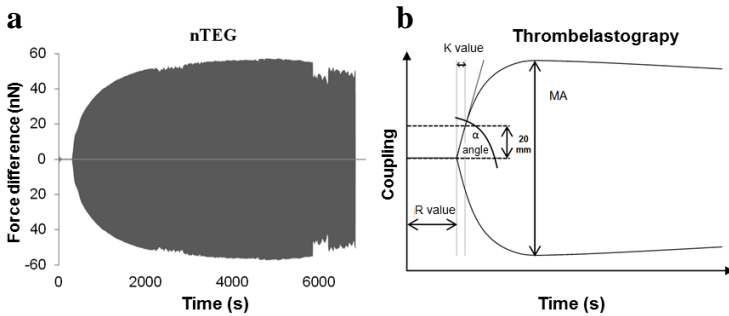


Fig. 3. Mirroring the nTEG curves on the x-axis results the nano-thrombelastogram (a). Schematic figure of a thrombelastogram indicating the characteristic parameters (b).

Both methods (TEG and nTEG) deliver valuable data of the mechanical properties of the three-dimensional fibrin network. If we disregard the meaning of our force difference curves and we evaluate the results only graphically, the characteristic time parameters (such as R and K values) can be compared with the TEG results. But while the amplitude signal of TEG measures the mechanical properties of the clot indirectly, the force difference [nN] and dissipated energy [J] of the nTEG

results well-defined physical parameters. The changes in the viscous and the elastic properties of the clot can be followed separately during the clotting process by the measuring the force difference and the dissipated energy. Compared with TEG, in nTEG the path of the movement is shorter and the applied shear force is much lower. Thus, small changes in the viscoelastic features that might be averaged out during TEG, can be followed with nTEG.

4.2 Fibrinolysis followed with nTEG. (T2)

The force difference and the dissipated energy started a decrease as a result of streptokinase (STK) induced lysis, and stopped around 0 value (**Fig. 4. part a**). The slope of the decrease corresponds to the speed of the lysis. The slope increased three times after the application of 3000 IU STK compared with 300 IU, but 6000 IU resulted no further increase, indicating a saturation around 3000 IU STK activity (**Fig. 4. part b**).

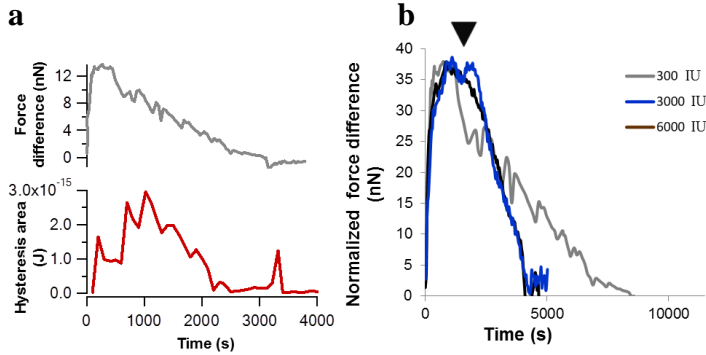


Fig. 4. Time-dependent evolution of force difference and dissipated energy values in a sample treated with 300 IU STK (a). Normalized force-difference curves upon STK treatment (b). STK was applied in different concentrations. Arrowhead indicates the time point of STK administration.

4.3 Preparation and morphology of a quasi-2D fibrin network. (T3)

Activation of fibrinogen with thrombin on mica surface in small volume resulted a quasi-2D structure after clotting and drying of the sample (**Fig. 5. part a, b**). The thickness of the network (z-dimension) is 5 orders of magnitude smaller compared with the width (x-y dimension) thus the thickness of the sample is negligible compared with its width and the sample is quasi-2D. In this quasi-2D structure, fibrin fibers are formed in a layer and the overlapping of the fibers still allows the analysis of the individual fibers. The formed quasi-2D meshwork is suitable for topological measurements such as AFM, and the width and the height of individual fibers can be analyzed (**Fig. 5. part c**).

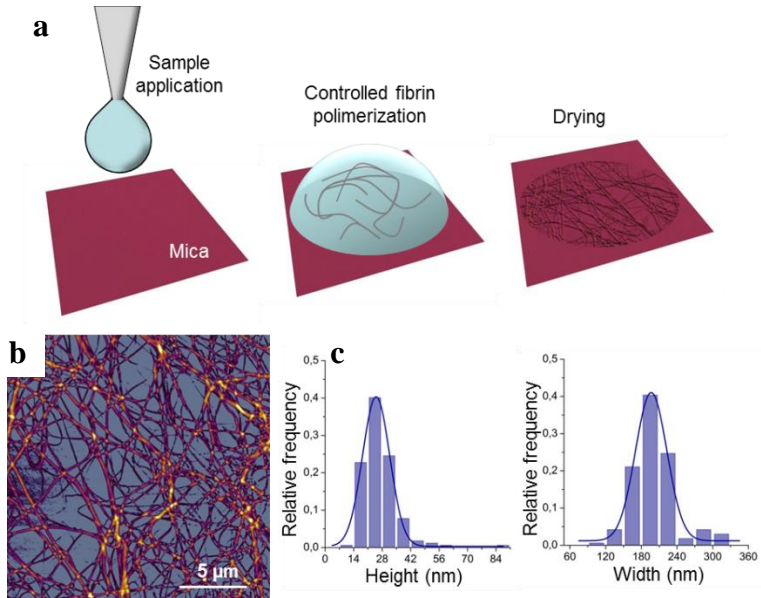


Fig. 5. Preparation of the quasi-2D fibrin network for AFM analysis (a). AFM image of the fibrin network (b) Histogram of the filament height and width (c) ($n=167$).

The drying of the sample after the clotting is a final stabilization step that fixes the sample on the mica surface. Without this step, the clot was washed from the surface and only fragments of the network were observable with further AFM analysis.

4.4 Tuning the quasi-2D fibrin network with thrombin activity and NaCl concentration.

Decreasing NaCl concentration have been shown to increase fibrin fiber diameter. In our quasi-2D fibrin network, the width and the height of the fibers increased,

when the clotting was initiated at lower NaCl concentration. We observed the similar overall effect in the case of thrombin: applying lower thrombin activity resulted higher and wider fibers (**Table 1**).

Table 1. Morphological parameters of fibers prepared at different NaCl and thrombin concentrations.

	Width (nm)	SD (nm)	Height (nm)	SD (nm)
1 IU thrombin	160	± 37.5	18	± 9.8
0,1 IU thrombin	177	± 43	26	± 8.2
0,01 IU thrombin	250	± 69.5	34	± 9.6
150 mM NaCl	153	± 30	21	± 7
75 mM NaCl	217	± 65	23	± 8
20 mM NaCl	242	± 70	28	± 8

4.5 Lysis of the quasi-2D fibrin network (T5)

We scanned the prepared quasi-2d fibrin network, lysed it with 3 nM plasmin for 30 min then washed, dried and scanned it again. We compared the AFM images before and after the lysis. The structure of the network is maintained after lysis. The global shape and the orientation of the fibers retained although most of the fibers became partially fragmented (**Fig. 6. parts a, b**). The topological height profile along a single fibrin fiber showed fluctuations as the result of the lysis, and it was not observable prior to lysis (**Fig. 6. part c**). The average height of the fibers decreased from 21 nm (± 8 nm SD, n=47) to 16 nm (± 7 nm SD, n=44), while the average width increased from 185 nm (± 47 nm SD, n=47) to 248 nm (± 137 nm SD, n=44) due to the lysis (**Fig. 6. parts d, e**). We calculated the significance of the changes with t-

probe. The p-value was smaller than 0.0001, so the changes caused by the lysis are considered to be significant.

For further evaluation of the decreased height and increased width we introduced a new parameter, the height/width ratio. This parameter decreased from 0,115 ($\pm 0,027$ SD, n=47) to 0,081 ($\pm 0,052$ SD, n=44) due to the lysis. The decrease was significant.

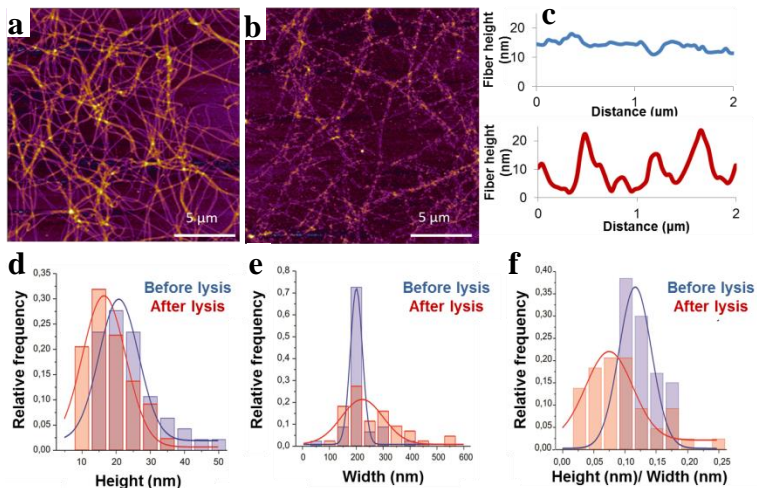


Fig. 6. Quasi-2D fibrin network before (a) and after (b) lysis. Topographical height profile along a single fiber before (blue) and after the lysis (red) (c). Histogram of the distribution of fiber height (d), width (e) and height/width ratio (f) prior to and after the lysis.

4.6 Fibrinolysis followed real time on a single fiber (T4)

We followed the nano-biophysical changes on a single fiber due to the fibrinolysis real time with high

resolution. The lysis proceeded 30 min long in the presence of 2,5 nM plasmin. In this time we could scan the fiber 20 times with Cypher ES AFM. The fiber first increased in height, then the initially straight fiber acquired local curvatures and attained an overall zigzag shape. Finally, the transection of the fiber occurred. We analyzed fiber height and width on each image along the cross-sectional profile marked with a red line on the first image (**Fig. 7. part a**). Not only the width but also the height of the fiber increased in the first phase of the lysis, indicating that the fiber volume has increased. Then the height and the width reached a plateau, and decreased abruptly (**Fig. 7. part b**).

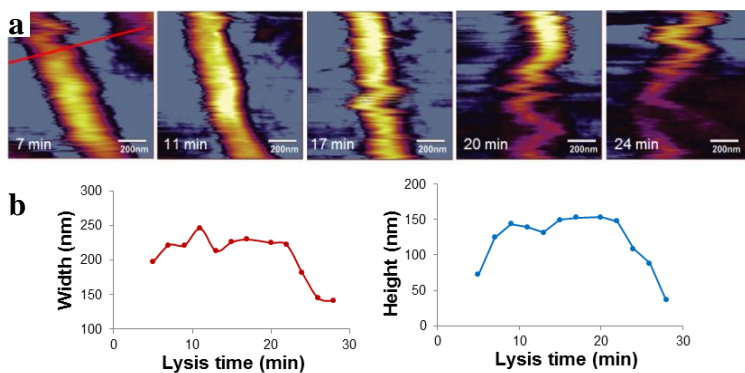


Fig. 7. Topographical changes of a fiber during lysis (a). Changes in the width and height of an individual fiber during lysis (b).

4.7 Model of plasmin-induced fibrinolysis (T4)

Based on the measured changes in the height and the width of the individual fibers during the lysis we can uncover the molecular mechanism of the process.

Fibrinolysis can be divided in two phases (Fig. 8). The first, initial phase takes a longer time and plasmin cleaves the interprotofibrillar interactions. That results a swollen, flexible fiber structure where the interprotofibrillar distance is increased. From the many plasmin cleavage sites on fibrin, the α C region is cleaved first. It results the cleavage of the lateral interactions and a swollen, flexible fiber structure. This first phase can have an important consequence on the lysis. Plasmin can diffuse inside the fiber and reach cleavage sites it couldn't reach before. This is followed by the second phase of the lysis, when the transection of the protofibrils occur rapidly, resulting the and axial fragmentation of the whole fiber.

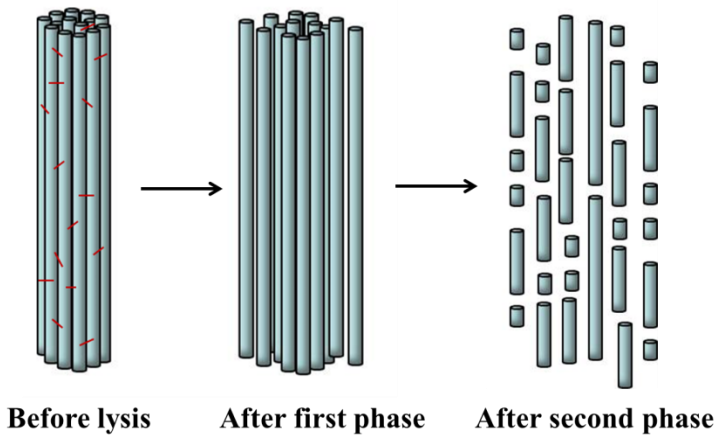


Fig. 8. Schematic model of the plasmin-dependent fibrinolysis.

5 Conclusion

In the present work I developed two methods, the nTEG and the preparation of the quasi-2D fibrin network that enables the investigation of the morphology and mechanical properties of the fibrin network on nanoscale.

With nTEG we followed the changes in the mechanical properties of the clotting plasma in real time. We characterized the changes in the elasticity of the clot with a well-defined physical parameter, the force difference [nN]. The curve representing the temporal changes of the force difference resembles well to the TEG curves, although the amplitude signal of the TEG only indirectly characterizes the mechanical properties of the clot. With nTEG the changes in the viscosity can also be followed and characterized by a well-defined physical parameter, the dissipated energy [J]. Changes in the viscosity can be due to the energy dissipation in the protein structure. The temporal changes of the viscous property were different from the changes of the elastic property. In the plasma clot both the force difference and the hysteresis area decreased due to the lysis induced by STK.

The preparation of the quasi-2D fibrin network from the 3D structure was reproducible. The method enabled the AFM analysis of the microstructure of the clot, as well as the analysis of the height and the width of individual fibers. The height and the width of the fibers can be tuned with the NaCl concentration or with the applied thrombin activity. The changes on the network due to the plasmin-driven lysis can be followed and analyzed and the structure of the individual fibers can be investigated on nanoscale. Based on our results the model of plasmin-dependent fibrinolysis is the following. The lysis can be divided in two phases. In the first phase the

fibers swell and become flexible due to the cleavage of interprotofibrillar interactions. In the second phase fibers are transected, leading to a rapid axial fragmentation of the fiber.

The new scientific accomplishments of my work are collected in the following points:

T1. I developed the nTEG method that provides insight to the time-dependent nanoscale changes in the viscous and elastic behavior of the 3D fibrin network during coagulation.

T2. With the nTEG method the nanoscale changes in the viscoelastic properties can be followed in STK-induced fibrinolysis.

T3. I developed a quasi-2D fibrin network for the structural investigation of the fibrin network and the individual fibers by AFM.

T4. We characterized the lysis by a two-phase model. In the first phase fibers loosen then in the second phase fibers go through a rapid axial fragmentation.

6 Publications of the candidate

6.1 Publications related to the thesis

- [1] Feller T, Hársfalvi J, Csányi C, Kiss B, Kellermayer M. (2018) Plasmin-driven fibrinolysis in a quasi-two-dimensional nanoscale fibrin matrix. 10.1016/j.jsb.2018.05.010. J Struct Biol. 2018 Sep;203(3):273-280. IF₂₀₁₇: 3,489

- [2] Feller T, Kellermayer MS, Kiss B. (2014) Nano-thrombelastography of fibrin during blood plasma clotting. 10.1016/j.jsb.2014.04.002 J Struct Biol. 2014 Jun;186(3):462-71. IF₂₀₁₄: 3.10